applied sciences

MDPI

Article

A Computational Study of Polymer Solutions Flow Regimes during Oil Recovery from a Fractured Model

Dmitriy Guzei *, Angelica Skorobogatova, Sofia Ivanova and Andrey Minakov *

Laboratory of Physical and Chemical Technologies for the Development of Hard-to-Recover Hydrocarbon Reserves, Siberian Federal University, 660041 Krasnoyarsk, Russia

* Correspondence: dguzey@sfu-kras.ru (D.G.); aminakov@sfu-kras.ru (A.M.)

Abstract: Increasing the efficiency of hydrocarbon field development is an important issue. One of the methods for increasing oil recovery is the injection of aqueous solutions of polymers. Although this method has been known and used for quite some time, further systematic research is needed to further improve its effectiveness. In this work, systematic computational studies of the features of oil displacement by aqueous polymer solutions from a naturally fractured structure were carried out. Direct numerical modeling of a two-phase immiscible flow in the process of displacing oil from a natural fracture structure using solutions of anionic polymers based on polyacrylamide was carried out. Aqueous solutions of three different polymers were considered, the concentrations of which varied from 0 to 0.1%, and the molecular weights were from 10 to 20 mln c.u. The rheological properties of polymers and their wetting characteristics have been previously studied in laboratory experiments. A distinctive feature of the polymers considered was the non-Newtonian nature of their aqueous solutions even at low concentrations. To take these processes into account, the computational technique has been extended to the case of non-Newtonian rheology for immiscible two-phase flow in one of the media. During numerical simulations, the effect of the concentration of polymers, their molecular weight, and charging density on the flow regimes in a fractured reservoir have been investigated systematically at various crude oil viscosities. It has been shown that the use of a 0.1% aqueous solution of polyacrymalide can increase the oil-recovery factor by 1.8 times. It has been established that, with an increase in the molecular weight and surface charge density of the polymer, the efficiency of its use for enhancing oil recovery increases. With an increase in the viscosity of the displaced oil, the effect of using the injection of the considered polymers also increases. The data obtained in this work can be used to further improve polymer-flooding technologies for oil fields.

Keywords: polymer flooding; carbonate reservoirs; fracturing; polyacrylamide solutions; numerical simulation; volume of fluid method

check for updates

Citation: Guzei, D.; Skorobogatova, A.; Ivanova, S.; Minakov, A. A Computational Study of Polymer Solutions Flow Regimes during Oil Recovery from a Fractured Model. *Appl. Sci.* **2023**, *13*, 11508. https://doi.org/10.3390/app132011508

Academic Editors: Jean-Michel Guenet, Paula Vasquez and Michael Cromer

Received: 16 August 2023
Revised: 14 October 2023
Accepted: 16 October 2023
Published: 20 October 2023

Copyright: © 2023 by the authors. Licensee MDPI, Basel, Switzerland. This article is an open access article distributed under the terms and conditions of the Creative Commons Attribution (CC BY) license (https://creativecommons.org/licenses/by/4.0/).

1. Introduction

Currently, acrylamide-based synthetic polymers have been widely used in oilfield development to enhance oil recovery. Today polymer flooding is one of the most efficient oil-recovery enhancement methods [1–3]. In most cases, partially hydrolyzed polyacrylamide is used for this process, since this is a relatively inexpensive and accessible reagent. In addition to its availability, other important advantages of polyacrylamides are their good solubility in water, due to which the viscosity of solutions quickly changes, the ability to easily filter in rock, and, also, environmental safety. However, these polymers have low stability in reservoir conditions, which are characterized by high temperature and increased salinity. An increase in temperature in the rock reservoir leads to the hydrolysis of polyacrylamide [4]. Another important problem with the use of polymer flooding with polyacrylamide solutions is their high sensitivity to the formation of water salinity. Anionic activity in the polymer chain in the presence of divalent calcium and magnesium cations leads to a decrease in the viscosity characteristics of the solution [5].

In addition, the problem of polymer adsorbing by rock walls is well known. Therefore, a large number of laboratory tests are now being carried out to increase the efficiency of polymer flooding. Therefore, the search for new, more thermally stable, polymer compounds is currently continuing. For example, experiments on the polymer flooding of a one-dimensional sandstone model using an aqueous solution high-molecular-weight hydrophobic-associated polyacrylamide copolymer (HAPAM) were conducted by El-hoshoudy et al. [6]. The rheological properties and thermal stability of HAPAM were investigated in detail. It was found that HAPAM has satisfactory thermal and salt resistance. This copolymer exhibits pseudoplastic behavior and is also capable of reducing the interfacial tension between the crude oil and the brine solution at room temperature, resulting in increased mobility of residual crude oil.

The process of injecting partially hydrolyzed polyacrylamide polymer (PHPA) into a rock model was experimentally investigated by Mishra et al. [7]. A sandy bulk model was used in the experiments. The experiments have shown that polymer behavior is influenced by polymer concentration, pH of the solution, and salinity. Increasing polymer concentration enhances oil recovery.

Li et al. [8] synthesized a synthetic water-soluble sulfonated polyacrylamide copolymer (SPAM), based on acrylamide with sulphonic acid groups and quaternary ammonium groups. A comparative analysis of the synthetic copolymer with the partially hydrolyzed polyacrylamide polymer (HPAM) was carried out. The synthetic copolymer has shown better thermal stability at high salt-ion concentrations, as well as demonstrating salt tolerance and shear stability. In core-flooding experiments, the oil-recovery factor (ORF) was higher when using SPAM as compared to that for HPAM.

In addition to synthetic polymers, xanthan gum is also used in the oil industry in large quantities, since it can be utilized in high-salinity solutions. In addition, it is also compatible with a great number of surfactants and other additives used for injection into the bed [9]. Using a xanthan gum solution as a polymer-flooding fluid was studied by Ghoumrassi-Barr et al. [10]. The authors studied the rheological properties of xanthan gum solutions; the rheology was accurately described by the Herschel–Bulkley and Ostwald models.

In addition, the modification of conventional polymer solutions by adding various-size nanoparticles and compositions is currently being investigated intensively [11–13]. In fact, this is a new area in oil-recovery enhancement methods. However, the use of nanoparticles and the evaluation of the effect of additives on oil recovery have not been sufficiently studied. In this connection, active research is being carried out in this direction. For example, adding silicon dioxide nanoparticles (SiO_2) into the polymer solutions, used for enhancing the oil-recovery factor by the polyacrylamide solutions, was suggested by Haruna et. Al. [14]. Studies have shown that the nanocomposites used are capable of forming agglomerations/deposits, which, consequently, leads to a decrease in the expected effect. In doing so, Hu et al. revealed that adding silicon oxide nanoparticles has a significant effect on the viscosity and viscoelastic properties of HPAM [15].

Along with a great number of laboratory experiments, numerical simulations are extensively carried out to study polymer flooding. In the field of numerical simulation of polymer flooding, the two following trends can currently be distinguished. One is treating the porous medium as a continuum with averaged properties and solving the Darcy equation for each phase under study, making the system geometry independent on a microscale [16–18]. The second approach is based on using the Navier–Stokes equation system over the whole complex network of microchannels in the porous medium. This approach could be beneficial for developing new displacement fluids and considering their effects at a microscopic scale. Subsequently, these studies should be supplemented by reservoir simulation at a certain scale and field testing using the Darcy equation approach. These studies are used mainly for terrigenous reservoirs with well-studied porosity and relative phase permeability.

In addition to works where Eulerian effective porosity methods are widely accepted, direct numerical simulation methods with phase-interface resolution [19,20] have recently

begun to be applied in computational studies of polymer flooding. However, at present, studies of polymer-fluid flow regimes during oil recovery using direct numerical simulation are still insufficient.

The conducted review has shown that most of the current research on the injection of polymers, as well as polymer solutions containing added nanoparticles, are associated with terrigenous reservoirs. However, there are also a significant number of carbonate fields with fractured reservoirs. To date, the number of studies on using polymer solutions in fractured reservoirs is quite low. Therefore, the effect of polymer solutions on oil-recovery enhancement in fractured reservoirs needs a systematic study conducted. Our work was the first to use a topology with naturally created fracturing, unlike other works in which synthetically generated structures that do not fully reflect the properties of real rocks are used to solve similar problems. To prepare a naturally cracked structure, an original approach was used, based on the evaporation of a suspension of nanodiamonds on a glass substrate. This made it possible to obtain a topology of the pore space close to the topology of real fractured cavernous rocks. A diagram showing the stages of the research described in the work is shown in Figure 1.

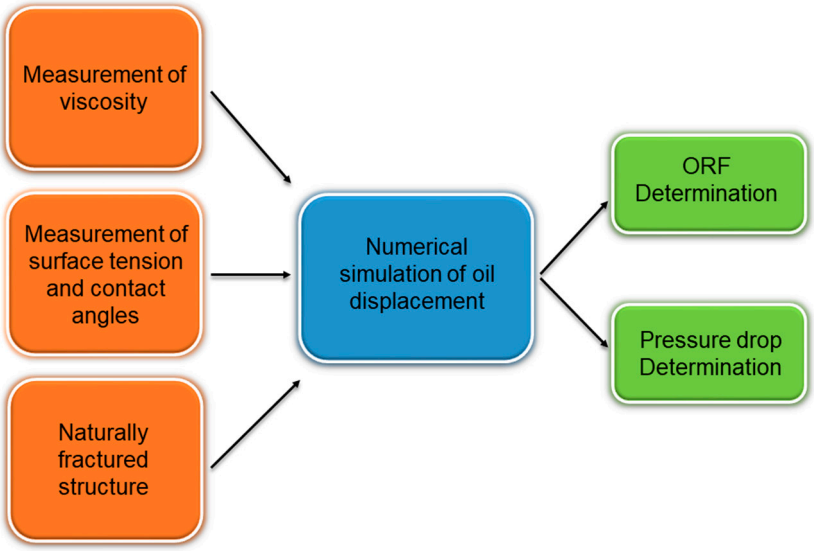

Figure 1. Flowchart of the study of oil displacement by aqueous solutions of polymers.

2. Materials and Methods

2.1. Investigation of the Properties of the Tested Fluids

Anionic polymers, based on polyacrylamide (PAA) of different grades were used in the present work, namely Praestol (2515, 2540) and Polyflock (A2020) with different molecular weights and charging densities. The 2515 and 2540 acrylic polymers had molecular weights of ~9 and 13 mln units, respectively. They also differed significantly in the surface charging density, equal to 10% for 2515 polymer and 30% for 2540 polymer. Polymer A2020 differed significantly from the others by a molecular weight equal to ~18 mln units and had a surface charging density of 20% (see Table 1). Molecular weight and charge data were provided by the manufacturer. Solutions with weight concentrations of 0.01, 0.5, and 0.1% were prepared. All polymer solutions used in the experiments were prepared using deionized water.

Table 1. Polymer characteristics.

Trademark	Molecular Weight, Million Units	Charge Density, %	Hydrolysis Degree, %	Bulk Density, kg/m^3	Manufacturer
Poliflok A2020	17–20	20	20	600–800	NPO Polyflok
Praestol 2515	8–10	10	-	550–750	CJSC Moscow-Stockhausen
Praestol 2540	12–14	30	-	600–750	CJSC Moscow-Stockhausen

The rheology of the aqueous polymer solutions was measured using a Brookfield DV2T rotary viscometer (ULA and LV-61 spindles). The reproducibility limit of the viscosity measurements does not exceed 0.5%, and the limits of allowable reduced error for ULA and LV-61 spindles are ±1% and ±2%, respectively. The measurement technique is described in detail in [21]. The measurements were carried out at 25 °C.

The dependence of viscosity on polymer concentration was investigated for A2020 aqueous polymer solutions. With the increasing polymer concentration, the viscosity changed as follows: increasing the concentration of A2020 polymer to 0.1% resulted in an increase in the dynamic viscosity coefficient μ (Figure 2). As can be seen, the aqueous polymer solutions exhibit a characteristic non-Newtonian behavior.

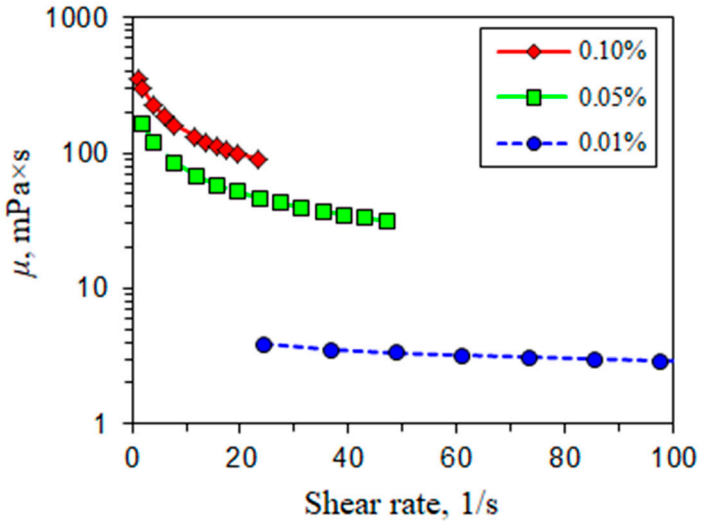

Figure 2. Dependence of dynamic viscosity of A2020 aqueous polymer solution on the shear rate at different concentrations.

As the polymer concentration in the solution increases, the change in the shear rate starts to have a greater impact on the viscosity. For a PAA concentration of 0.01%, the dependence of viscosity on shear rate is less pronounced compared to that for concentrations of 0.05 and 0.1%.

Since the viscosity of the solutions under study depends on the shear rate, the rheological characteristics of the polymer solutions were investigated. It was shown that the viscosity is well described by a power rheology law $\mu(\dot{\gamma}) = K\dot{\gamma}^{(n-1)}$. Increasing the polymer proportion in the solution significantly affects the rheological characteristics (consistency index K and flow-behavior index n), which are shown in Table 2.

Table 2. Rheological parameters of aqueous solutions on weight concentration of A2020 polymer.

wt.%	*n*	*K*, mPa×s
0	1.00	0.89
0.01	0.8103	5.60
0.05	0.4556	258.6
0.1	0.5016	440.5

The viscosity of the solutions changes significantly with the increasing polymer weight concentration, namely, the higher the polymer fraction, the higher the viscosity. As the polymer concentration increases, the flow-behavior index in the power model decreases, while the consistency index, on the contrary, increases. Thus, the non-Newtonian pseudo-viscoplastic properties enhance with the increasing concentration of the A2020 polymer additive.

The viscosity of aqueous polymer solutions of different molecular weights and charging densities with a weight concentration of 0.1% was measured as a function of shear rate. With increasing shear rate, the viscosity of the 0.1% concentration solutions decreased for all polymer samples tested (see Figure 3). This dependence is most pronounced for the 2540 polymer, while the viscosity of the 2515 polymer changes insignificantly while varying the shear rate. Thus, all the solutions exhibit non-Newtonian behavior.

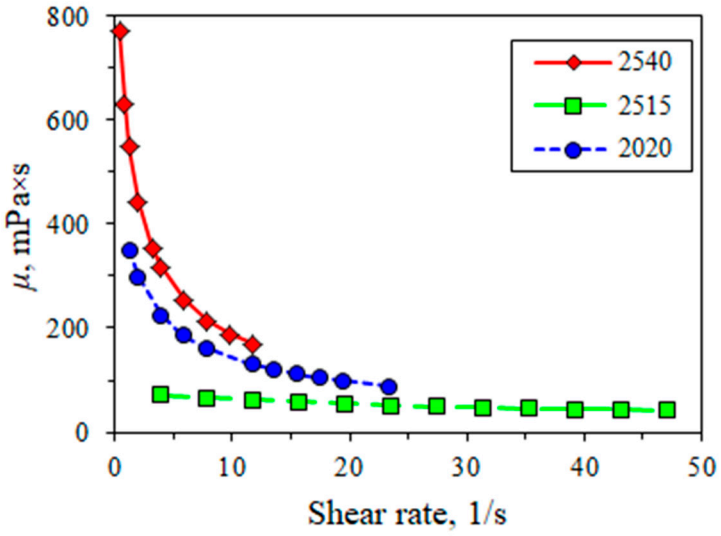

Figure 3. Dependence of the dynamic viscosity of polymer solutions on the shear rate.

A study of the rheological characteristics of 0.1% solutions of different polymers has shown that the viscosity was higher for 2540 polymer, while the flow-behavior index for this polymer grade was the lowest. Polymer 2515 had the lowest viscosity at a concentration of 0.1%, while its flow-behavior index was higher than that of the other solutions. A comparison of the rheological parameters is shown in Table 3.

Table 3. Rheological parameters of different polymer grades.

Polymer Grade	*n*	*K*, mPa×s
2540	0.49103	609.56
A2020	0.50166	440.57
2515	0.72708	120.99

It was found that when increasing the charging density and molecular weight of the polymer, the effect of the additive on the viscosity and rheology of the solution increased. Moreover, at close molecular weights, the effect of polymer addition was stronger the higher the charging density.

The interfacial tension σ of the boundary of an aqueous solution of the polymer oil and the wetting angle θ were investigated using the technique, which was employed earlier [22]. A CoreLab TEMCO IFT-820-P hanging drop surface-tension measurement system was used to measure interfacial tension. The IFT cell operates at pressures of up to 68.95 MPa and temperatures of up to 176 °C. Within this range, most reservoir conditions can be accurately and safely simulated. This allows experiments to be carried out in an oxygen-free atmosphere. The contact angle and interfacial tension were both measured using the DropImage Advanced ver. 2.5.02 software (Ramé-Hart Instrument Co., Succasunna, NJ, USA). All surface tension and contact-angle measurements were performed at atmospheric pressure and 25 °C.

Figure 4 shows photos of experiments to determine the effect of A2020 polyacrylamide concentration on the wetting angle.

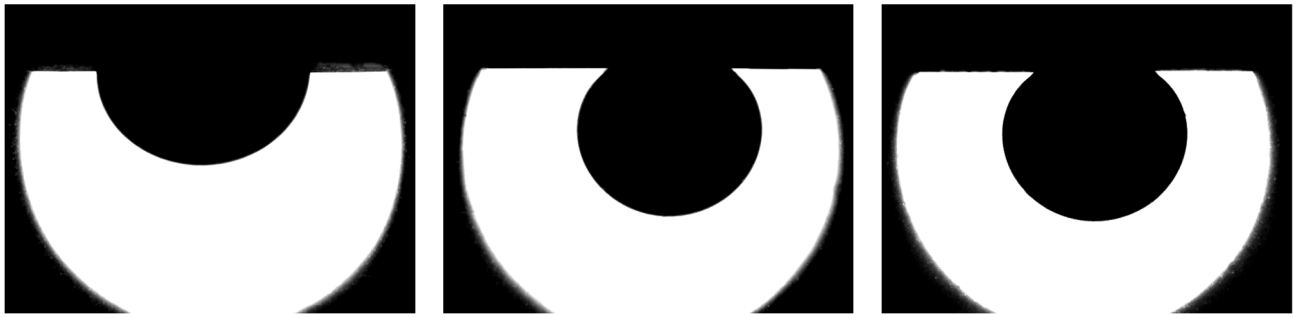

(**a**) (**b**) (**c**)

Figure 4. Photos of an oil drop on the rock in water (**a**), 0.05% A2020 polymer solution (**b**), and 0.1% polymer solution (**c**).

The interfacial tension was determined based on the geometric dimensions of the drop. Figure 5 shows photographs of an oil drop in water and in A2020 polymer solutions of 0.05 and 0.1% concentrations.



(**a**) (**b**) (**c**)

Figure 5. Photographs of an oil drop in water (**a**), 0.05% A2020 polymer solution (**b**), and 0.1% polymer solution (**c**).

The results of determining the wetting angle of the system consisting of displacing fluid, oil, and rock, as well as the interfacial tension of the system consisting of displacing fluid and oil, are presented in Table 4.

Table 4. Wettability and interfacial tension characteristics of displacing fluids.

Displacing Fluid	Material	Concentration, %	θ, deg	σ, mN m
Water		-	105.7	29.9
p-p	2515	0.1	154.8	31.6
p-p	2540	0.1	161.1	30.4
p-p	A2020	0.05	159.0	30.1
p-p	A2020	0.1	158.6	30.6

The interfacial tension at the interface of polymer solutions with oil increased slightly compared to that for water. Adding polymer had a more significant effect on the wetting angle. The wetting angle increased (due to increased hydrophilicity) from 105 to 161° with the increasing polymer concentration. Wettability was most affected by the addition of a 2540 polymer with a charging density.

2.2. Fabrication of a Fractured Structure

We have used natural cracked surfaces to fabricate the fractured structures on the chip. For this purpose, an aqueous suspension with diamond nanoparticles with an average size of 5 nm and a concentration of 4 vol.% was prepared. The suspension was prepared using distilled water at 25 °C. TEM images of diamond powders are shown in Figure 6a. Nanoparticles were added to the base liquid, then mechanically mixed and subjected to ultrasonic treatment to break up particle conglomerates. Stirring with a high-speed mixer was carried out for at least 30 min until a visually homogeneous suspension was obtained. The viscosity of the suspension was 5 mPa×s. During ultrasonic treatment, the container with the prepared suspension was placed in a thermostat to maintain a constant temperature (25 °C). Ultrasound treatment was carried out at a frequency of 22 kHz. Ultrasound treatment occurred for 40 min. The suspension was dried in a glass Petri dish at 50 °C. Drying was carried out in air at atmospheric pressure until the change in the mass of the Petri dish ceased. A film formed on the bottom of the Petri dish and cracked naturally during the final stages of drying. Due to poor adhesion to glass, some of the film flakes peeled off, imitating the presence of cavities in the rock filled with oil. The structure contained both open cracks incorporated into a single network, and those closed on one side. Cracks closed on both sides were also present, some of which were removed during processing because they did not communicate with the main network. The minimum channel width was 50 μm, the average width was 110 μm, and the maximum cavity cross-section was 500 μm. A photograph of the resulting structure is shown in Figure 6b. In Figure 6b, the black color corresponds to the resulting films of nanosized diamonds, covered with a network of cracks (white color) with the inclusion of large voids where the coating of particles has peeled off.

The formed structure was scanned with stereoscopic microscope NSZ-608 Lomo with a digital camera of 20 MPix. The obtained raster image was vectorized using Inkscape graphic editor. Vector image, obtained after vectorization, was used to create the computational domain configuration for carrying out the numerical study.

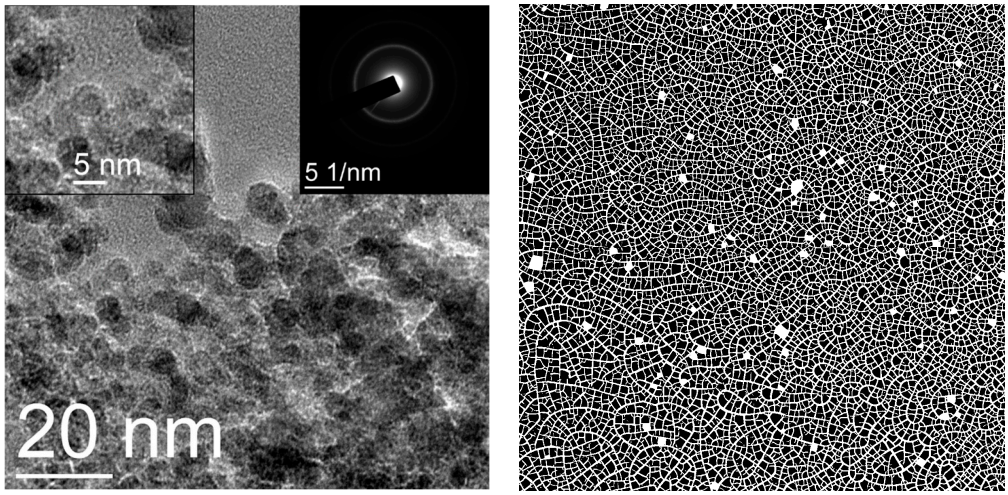

(**a**) (**b**)

Figure 6. TEM images of diamond powders (**a**) structure, obtained after drying an aqueous suspension of nanodiamonds (**b**).

2.3. Numerical Procedure

Direct numerical simulations were used to investigate two-phase flows during oil recovery from a fractured structure. A two-phase flow of immiscible fluids, namely oil and aqueous polymer solution, was considered. At present, there is a quite large number of methods for calculating such kinds of flows; however, for direct numerical simulation of two-phase flows in microchannels, the Eulerian methods are mainly used, such as the volume of fluid method (VOF) [23] and the Level set method [24]. This is primarily due to the dominant role of capillary forces and interactions of two-phase flows with the walls in microchannels. In this work, preference was given to the VOF method, which is characterized by high persistence of the numerical solution. This is very important when simulating flows in an extended network of microchannels at low capillary numbers.

The basic equations of the mathematical model within the VOF method are as follows:

$$\frac{\partial \rho}{\partial t} + \nabla\left(\rho \cdot \vec{V}\right) = 0, \tag{1}$$

$$\frac{\partial}{\partial t}\left(\rho \vec{V}\right) + \nabla \cdot \left(\rho \vec{V} \vec{V}\right) = -\nabla p + \nabla \cdot (\tau) + \vec{F}_s, \tag{2}$$

$$\frac{\partial \alpha}{\partial t} + \nabla \cdot \left(\alpha \vec{V}\right) = 0, \tag{3}$$

where α is the volume fraction of polymer aqueous solution in the computational cell, $\vec{F}_s$ is the volume force of interfacial tension at the oil–water interface, $\vec{V}$ is the flow velocity, p is the pressure, ρ is the density, and τ is the viscous stress tensor.

Within the direct numerical simulation method, the density is found as follows:

$$\rho = \rho_{\mathrm{p}} \alpha + (1 - \alpha)\rho_{\mathrm{o}}, \tag{4}$$

where ρ_{p} is the density of the aqueous polymer solution. Since the polymer concentration is very low, the density does not differ from that of pure water; ρ_{o} is the density of crude oil.

As can be seen from the viscosity measurement results, presented in the previous section, even at low concentrations, the polymer solution is non-Newtonian. The considered polymer solutions are characterized by a pseudo-viscoplastic rheology.

To simulate the rheological behavior, in this work, the generalized viscosity approach of the medium was used [25]. According to this approach, viscous stresses are defined as follows:

$$\tau_{ij} = \mu(\varphi, \dot{\gamma})\left(\left(\nabla\vec{V} + \nabla\vec{V}^{T}\right) - \frac{2}{3}\nabla\cdot\vec{V}E\right), \quad (5)$$

where $\mu(\varphi, \dot{\gamma})$ is the effective viscosity coefficient of the polymer solution, which depends significantly on the polymer concentration φ and the shear rate $\dot{\gamma}$, and E is the unit tensor.

Within the VOF method, the expression for the effective viscosity is:

$$\mu(\varphi, \dot{\gamma}) = \mu_p(\varphi, \dot{\gamma})\alpha + (1 - \alpha)\mu_o, \quad (6)$$

where $\mu_p(\varphi, \dot{\gamma})$ is the dependence of effective viscosity of a polymer solution on the polymer concentration and shear rate; μ_o is the viscosity of crude oil.

Experimental data have shown that the viscosity of the polymer solution is well described by the power-law model:

$$\mu_p(\varphi, \dot{\gamma}) = K(\varphi)\dot{\gamma}^{(n(\varphi)-1)}. \quad (7)$$

Dependences of rheological parameters $n(\varphi)$ and $K(\varphi)$ on the polymer concentration are shown in Table 2.

In addition to the rheology, the addition of polymer has a significant effect on the wettability and interfacial tension (see Table 4). The interfacial tension force $\vec{F}_s$ was determined as follows [26]:

$$\vec{F}_s = \sigma(\varphi)\nabla\left(\frac{\nabla\alpha}{|\nabla\alpha|}\right)\nabla\alpha. \quad (8)$$

The dependence of the interfacial tension coefficient $\sigma(\varphi)$ on the polymer concentration is shown in Table 4.

Except for fluid properties, such as viscosity and interfacial tension, the flow regimes in a fractured structure are critically influenced by the wetting conditions at the walls. By changing the wetting angle at the channel wall, one can significantly alter or shift the certain regimes of oil–polymer flows. The dependence of the wetting angle at the walls of the fractured structure $\theta(\varphi)$ was set directly from the experimental data presented in Table 4.

The system of equations described above has been solved by means of the control-volume technique. The convective flows were approximated using a second order counter-flow scheme. The approximation of the nonstationary terms was carried out in an implicit manner with the second order of accuracy. The solution to the transport Equation (3) has been carried out by a geometric interface reconstruction scheme. The commercial software product Ansys Fluent 2021R2 was used for calculations.

2.4. Problem Statement and Boundary Conditions

The computational study was carried out in a two-dimensional isothermal formulation. The geometry of the computational domain is shown in Figure 7a. This geometry was obtained by digitizing the image of a fractured surface. In Figure 7, the channels in which fluid flow occurs are filled with green, and the areas of solid rock are filled with white. A computational mesh with a total number of computational nodes of 700,000 has been constructed for the obtained geometry of the fractured medium. A fragment of the computational mesh in the channels is shown in Figure 7b.

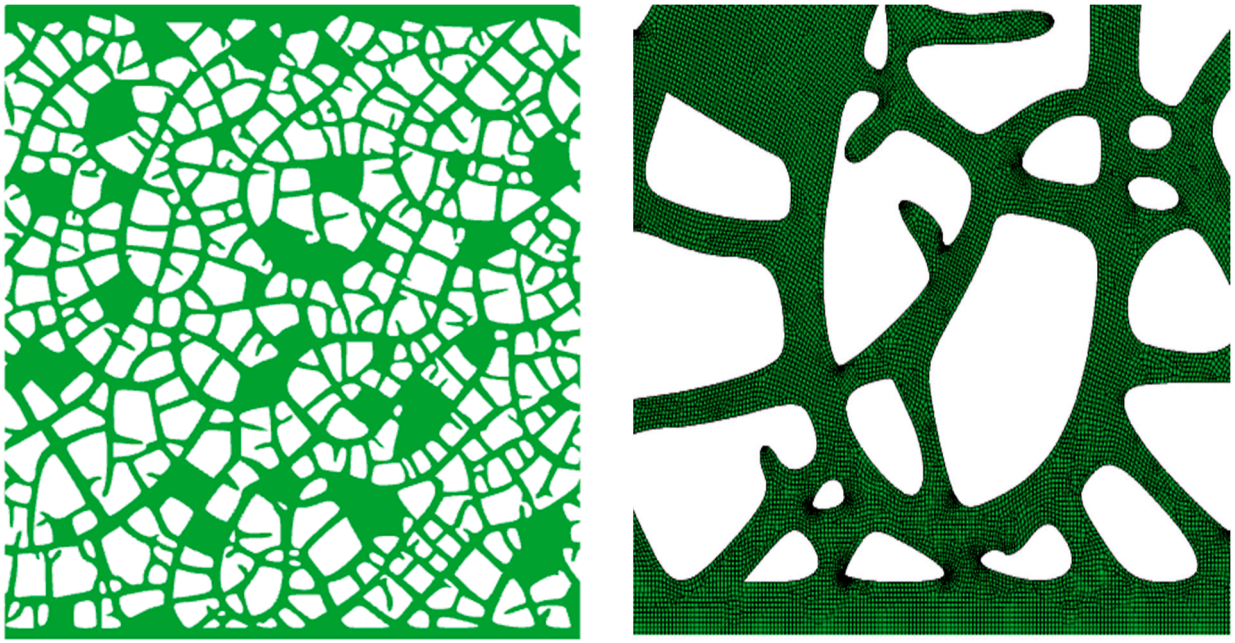

(**a**) (**b**)

Figure 7. Geometry (**a**) and fragment of the computational mesh (**b**).

A constant flow velocity, corresponding to the required capillary number, was set at the inlet. Neumann boundary conditions were set at the outlet. The wetting angle at the walls of the computational domain was determined experimentally. Experimentally determined interfacial tension coefficients and wetting angles for the system consisting of displacing agents, oil, and rock were also introduced into the computational model. The displacing agents considered in the experiments were water and polymer solutions.

Rheological parameters of the polymer solutions were determined experimentally. The viscosity of all polymer solutions used is described by a power rheology model with good accuracy.

At the initial time point, the entire computational domain was filled with oil. In this work, for definiteness, we used the approximation of zero initial water saturation. We carried out a detailed study of the influence of initial water saturation on displacement characteristics earlier [27]. The calculations resulted in determining the oil-recovery factor and pressure loss while injecting the polymer solutions into the fractured structure.

3. Results and Discussion

3.1. Influence of Polymer Concentration on Oil-Displacement Process

The influence of concentration on the oil-displacement efficiency and pressure drop has been studied for aqueous polyacrylamide solutions. Calculations were carried out for a capillary number equal to 4×10^{-5}, which corresponded to the displacement-agent velocity of 1.25×10^{-3} m/s, set at the inlet. Calculations were conducted for oil with a density of 900 kg/m^3 and a viscosity of 0.1 Pa×s. The density and viscosity of the oil were measured at 25 °C.

The study of the effect of the polymer concentration was carried out for a polyacrylamide polymer with a molecular weight equal to ~18 mln c.u. at weight concentrations of 0.05 and 0.1%.

During the numerical study of the displacement process, distribution patterns of the displacing agents and oil phases in the computational domain were obtained. The displacing agents used were water and polyacrylamide solutions with polymer weight concentrations of 0.05 and 0.1%. Figure 8 shows the distribution patterns of these displacing

agents depending on the displacement time; blue shows areas filled with oil, red shows areas filled with a displacing agent, and white shows rock areas.

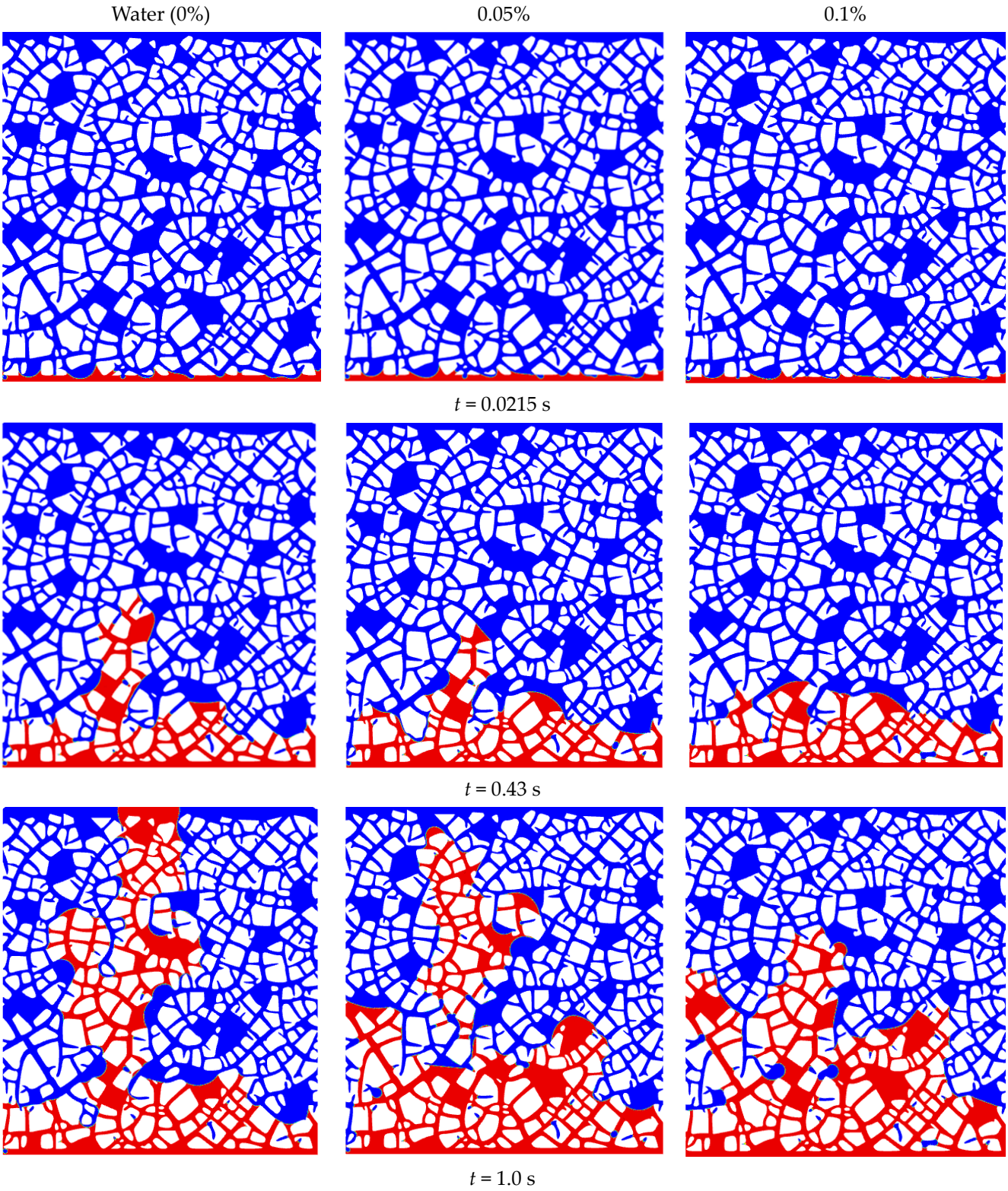

Figure 8. *Cont.*

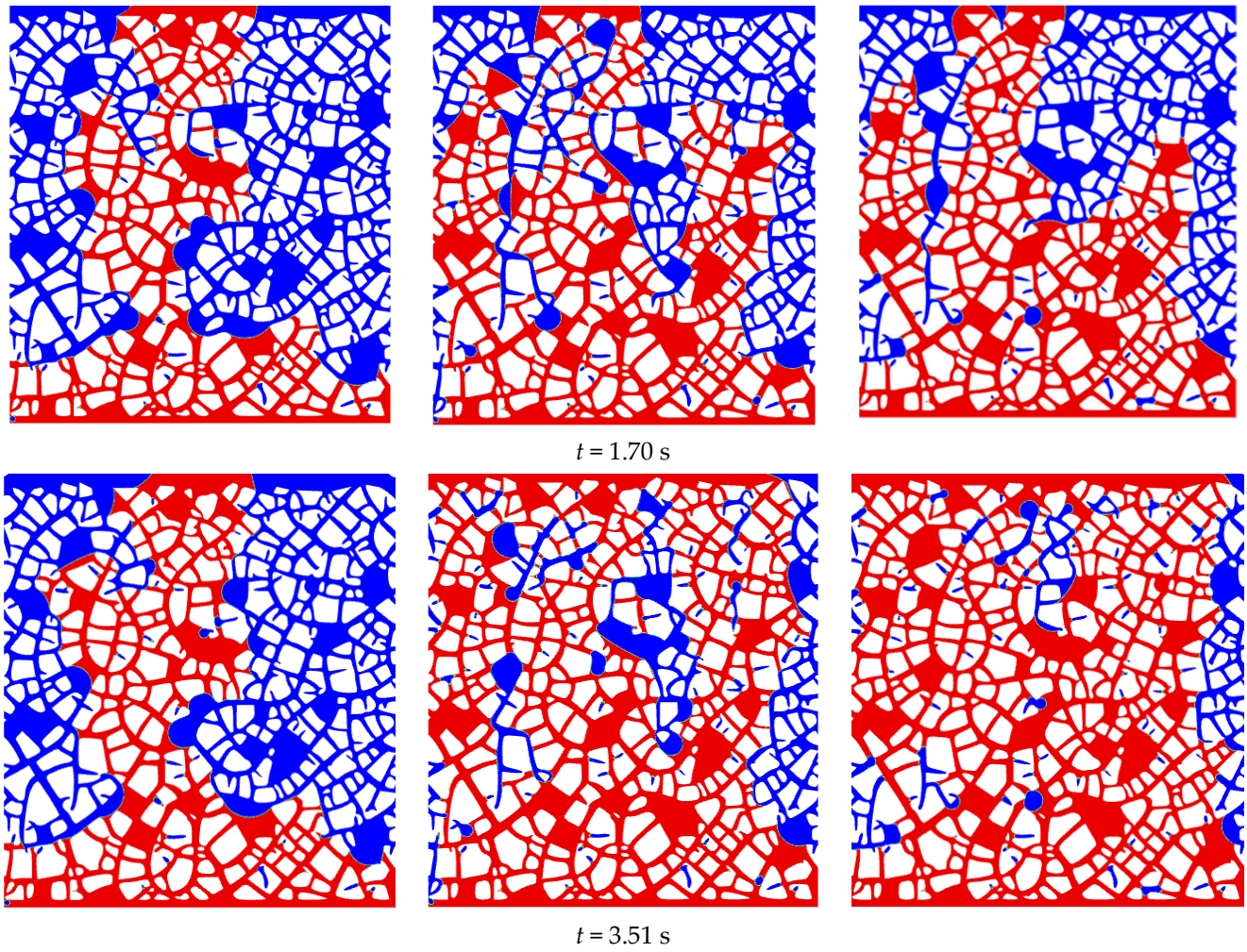

Figure 8. Phase distribution of the displacing agent and oil in a fractured medium during the displacement process. Effect of polymer concentration.

As can be seen from the phase distribution patterns presented in Figure 8, when displaced with water, oil is displaced in a rather narrow region of the model. During the displacement process, a "channel" is formed through which water continues to filter, leaving large areas filled with oil. The use of polymer solutions leads to an expansion of the displacement front compared to water, and, thus, additional areas of the fractured medium are involved in the process of oil displacement. With an increase in the concentration of the polymer solution from 0.05% to 0.1%, this effect intensifies.

The main mechanism of influence of the molecular weight and surface charge density of an acrylic polymer is a change in the rheological characteristics of its aqueous solutions. As shown in Table 1, all other things being equal, with an increasing mass concentration of the polymer in an aqueous solution, the viscosity of solutions changes significantly (the higher the polymer content, the higher the viscosity). As the polymer concentration increases, the flow-behavior index of the power-law model decreases. It was found that with increasing charge density and molecular weight of the polymer, the influence of the additive on the viscosity and rheology of the solution increased. The higher the molecular weight and charge density of the polymer, the lower the flow-behavior index and the more pronounced the non-Newtonian properties of solutions are. The non-Newtonian properties of solutions significantly affect the characteristics of their flow and the efficiency of oil displacement. With a decrease in the flow-behavior index n of the rheological model, a significant change in the velocity field in the channels of the porous medium occurs. An analysis of the distribution of viscosity of aqueous solutions in channels of a porous

medium at different polymer concentrations shows that the viscosity of solutions decreases greatly from the centers of the channels to the walls. Moreover, with a decrease in the flow-behavior index, this effect intensifies. This is due to the fact that, when approaching the walls, the shear rate increases significantly, and, consequently, the viscosity decreases. This influence of the non-Newtonian properties of polymer solutions with an increase in their concentration leads to a flattening of the velocity in the channels and the appearance in its center of the so-called quasi-solid flow region. Due to the fact that the velocity values in the central part of the channel decrease, and the fluid flow rate is fixed, the velocity increases in the wall part of the channel. This is shown in Figure 9. It can be seen that, with the increasing polymer concentration, the velocity field becomes more uniform. In addition to increasing the viscosity of the solution, increasing the velocity near the channel walls also improves oil recovery.

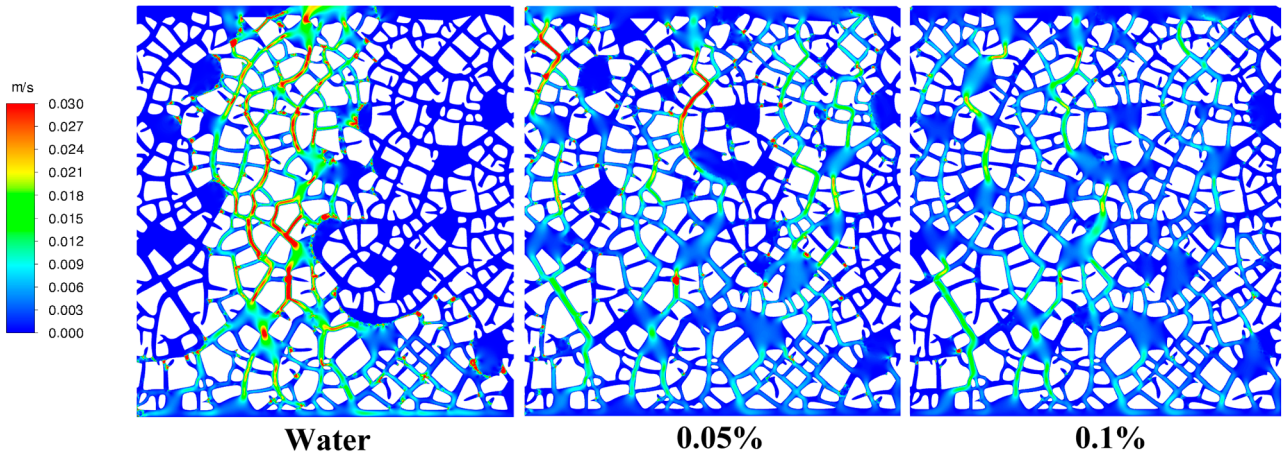

Figure 9. Velocity fields during the flow of water and polymer solutions with different concentrations.

To quantify the oil-displacement process from a fractured medium, in the course of conducted calculations, the dependence of the oil-recovery factor on the displacement time was obtained. This dependence is shown in Figure 10a for water and two concentrations of polymer. Subsequently, the oil-recovery factor (ORF), obtained from the calculation results of displacement, was constructed depending on the polymer concentration (see Figure 10b); zero concentration on the graph corresponds to water. Figure 10b shows the steady-state ORF values at time 6s, the color of the symbols corresponds to the lines in Figure 10a. As can be seen from the graphs shown in Figure 10a,b, using polymer solutions enhances the oil-recovery factor from a fractured medium from 0.45 (when displaced by water) to 0.74 when displaced by a polymer solution with a weight concentration of 0.05%. A further increase in the concentration to 0.1% leads to enhancing the oil-recovery factor to 0.85. Such a significant enhancement of the ORF is due to the fact that the viscosity of polymer solutions increases significantly compared to that of water, and also that these solutions are non-Newtonian fluids (whose viscosity coefficient depends on the shear rate). The displacement front for polymer solutions is wider in comparison with that for water. When displaced by water, the viscosity of water is lower than the oil viscosity, while for polymer solutions, the effective viscosity at low shear rates turns out to be comparable to the oil viscosity.

Changing the viscosity of the displacing agent leads to an increase in the pressure drop during the oil displacement from the fractured medium. In the course of calculations, we obtained the dependences of the pressure drop in a fractured medium when displaced by water or polymer solutions with different concentrations. Figure 11a shows the time dependence of the pressure drop in a fractured medium during displacement by various displacing agents. To simplify the comparison of the pressure drops when using water or polymer solutions of different concentrations, the dependence of the averaged pressure

drop at the steady-state section was constructed when the oil-recovery factor values did not change. The dependence of the steady-state pressure drop on the weight concentration of the polymer is shown in Figure 11b, the color of the symbols corresponds to the lines in Figure 11a. As can be seen from the graphs presented, using polymer solutions significantly increases the pressure drop used on injection in the steady-state area. Thus, for a polyacrylamide solution with a concentration of 0.05%, the pressure drop increases by seven times compared to that for water. With an increase in concentration to 0.1%, the pressure drop increases by 10.8 times relative to that when displaced by water.

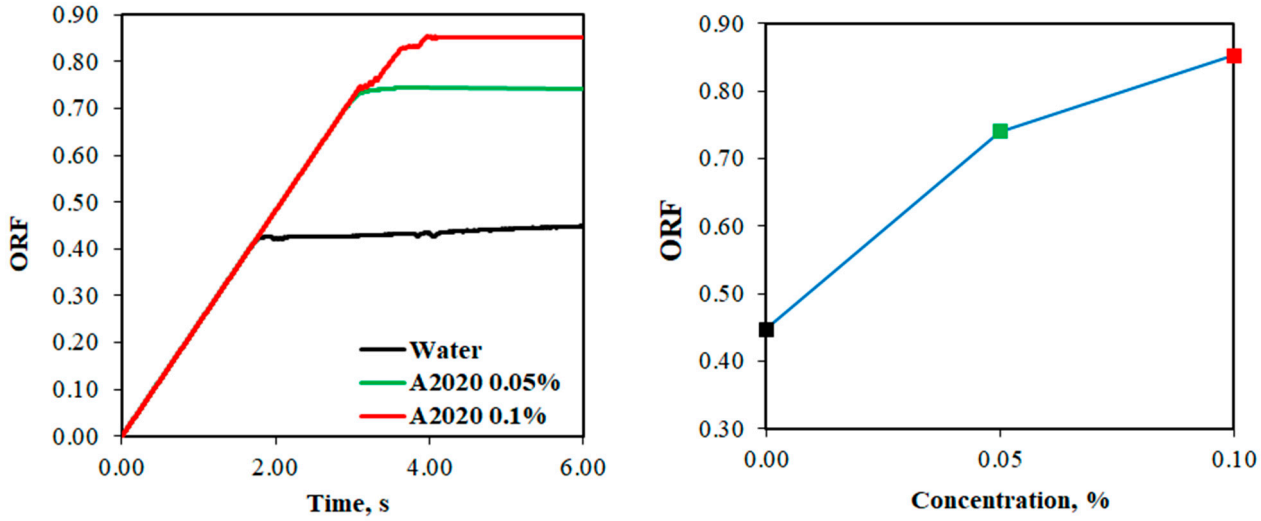

Figure 10. Oil-recovery factor vs. time (**a**), and the overall oil-recovery factor vs. concentration of the polymer solution (**b**).

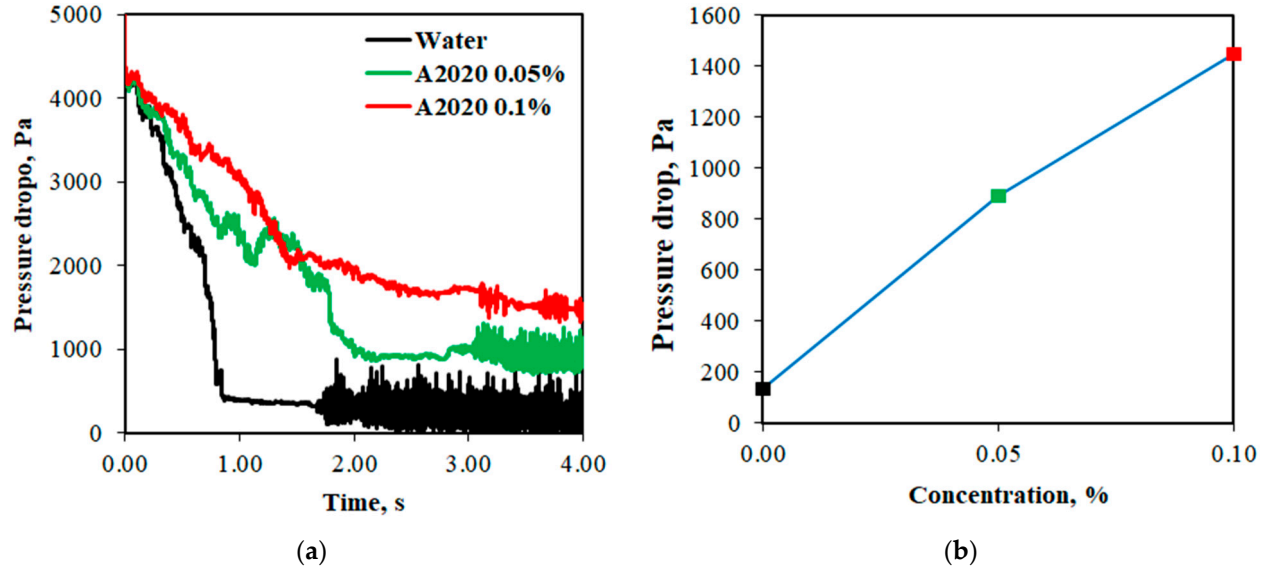

Figure 11. Pressure drop vs. time (**a**), and the averaged pressure drop at steady flow mode vs. polymer concentration (**b**).

The analysis of the breakthrough time of the displacement agent through a fractured medium filled with oil was carried out during the calculations. Figure 12 shows the breakthrough time of the displacing agent depending on the weight concentration of polyacrylamide. With an increase in the polymer concentration, the breakthrough time

increases. Thus, the breakthrough time for water is 1.67 s, while for 0.05% polymer solution, the breakthrough time is already 2.9 s. The breakthrough time of the displacing agent increases to 3.17 s at a concentration of up to 0.1%, which contributes to the recovery of an additional amount of oil. The increase in the breakthrough time is due to the high viscosity of polymer solutions and the formation of a wider displacement front, unlike water, which breaks through a narrow region of a fractured medium.

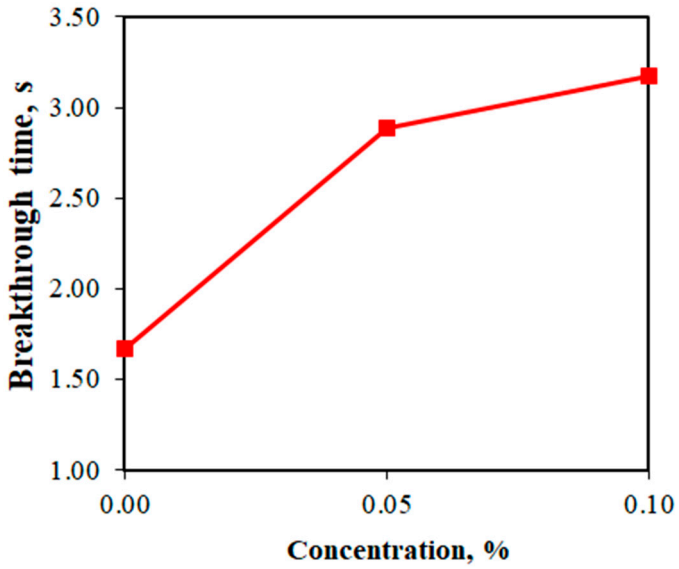

Figure 12. Breakthrough time vs. polymer concentration.

3.2. Investigation of the Effect of Polymer Solution Properties on Oil-Recovery Factor

The effects of the polyacrylamide solution properties on the ORF and pressure drop have been studied. Three polyacrylamide polymer solutions with a weight concentration of 0.1% were considered; grades 2515, 2540, and 2020 polymer solutions with relative molecular weights of ~9, ~13, and ~18 mln c.u. were considered in the computational study. The wetting angle and the surface tension, as well as rheological parameters, were experimentally determined for all polymer solutions considered. The calculations were performed for a capillary number of 4×10^{-5}. Calculations were carried out for oil with a density of 900 kg/m^3 and a viscosity of 0.1 Pa×s.

Based on the calculation results, the phase distributions of the displacing agents and oil in the computational domain were obtained when displaced by three solutions of polyacrylamide with different molecular weights and the same concentration. Figure 13 shows a comparison of the distribution patterns of oil and displacing agents in the pore space for different points in time. Blue color shows the pore space filled with oil, red is the displacing agent, and white color corresponds to solid rock.

To quantify the process of oil displacement from a fractured medium, the dependences of the ORF on the displacement time were obtained during the calculations. These dependences for water and the three polyacrylamide solutions are shown in Figure 14. For grades 2515, 2020, and 2540 polymer solutions with different molecular weights, the oil-recovery factors, obtained during calculations, were equal to 0.863, 0.85, and 0.88, respectively. Such close values of the oil-recovery factors were obtained due to a strong increase in the viscosity of polymer solutions at a concentration of 0.1%.

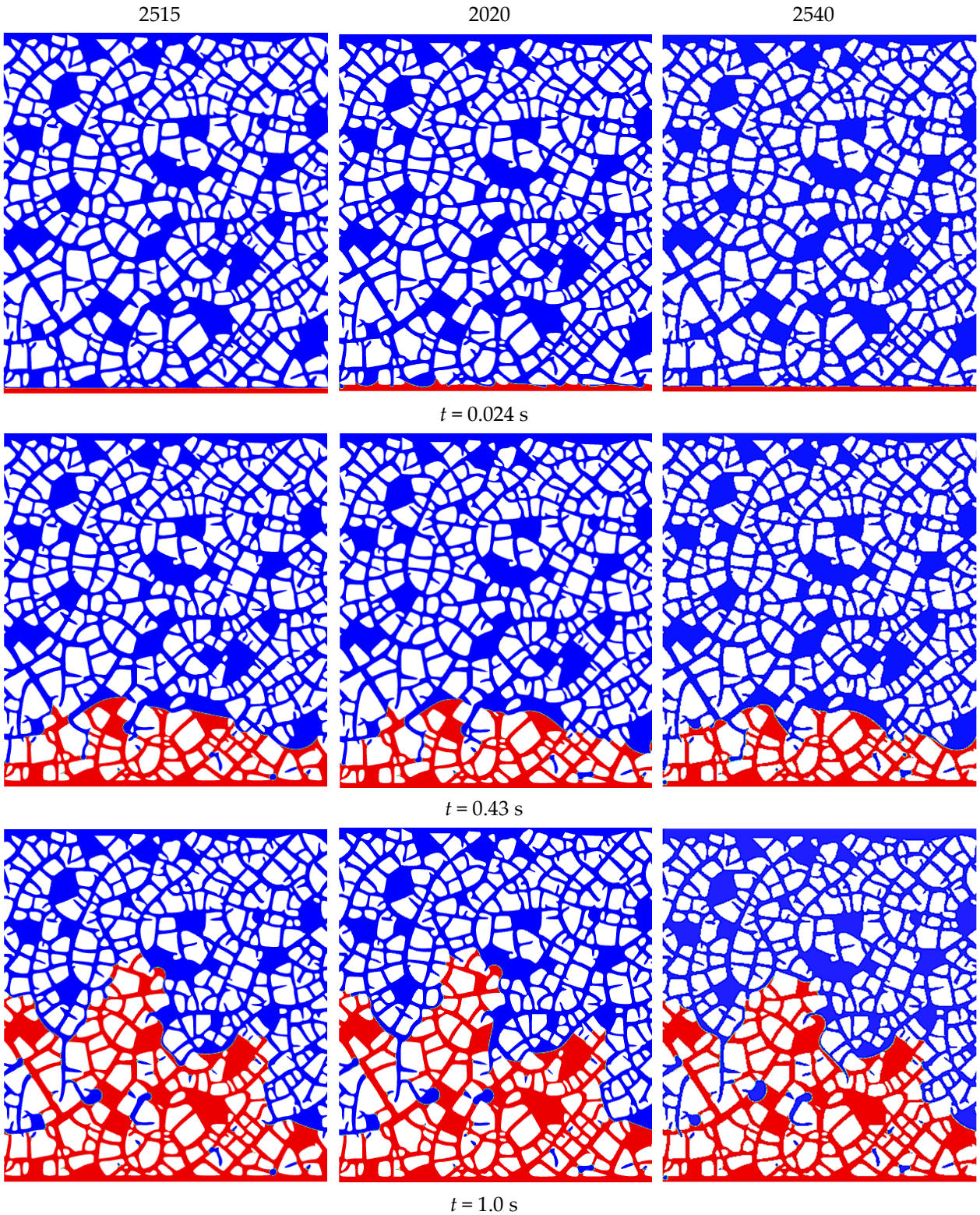

Figure 13. *Cont.*

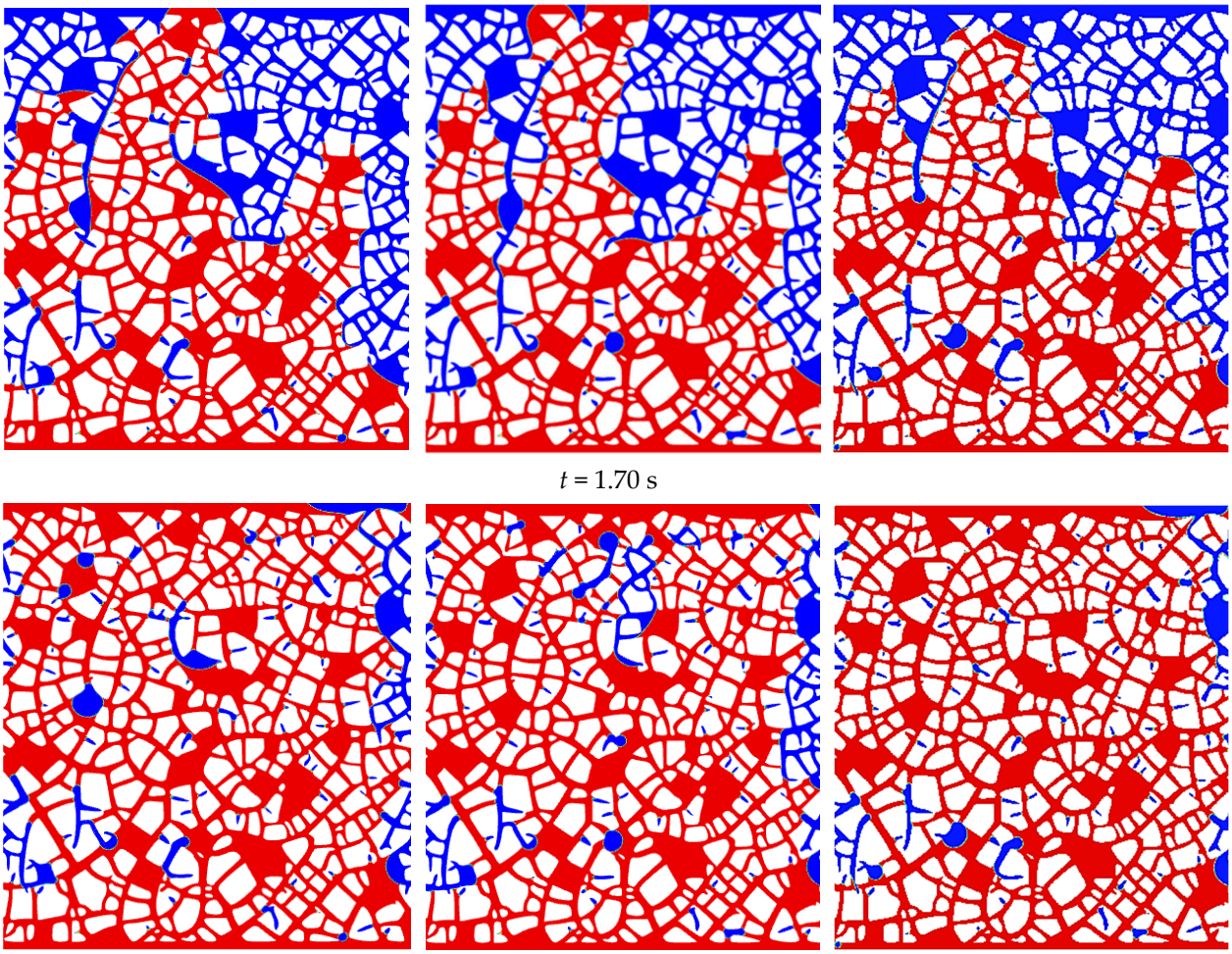

Figure 13. Phase distribution of the displacing agent and oil in a fractured medium during the displacement process. Effect of polymer solution properties.

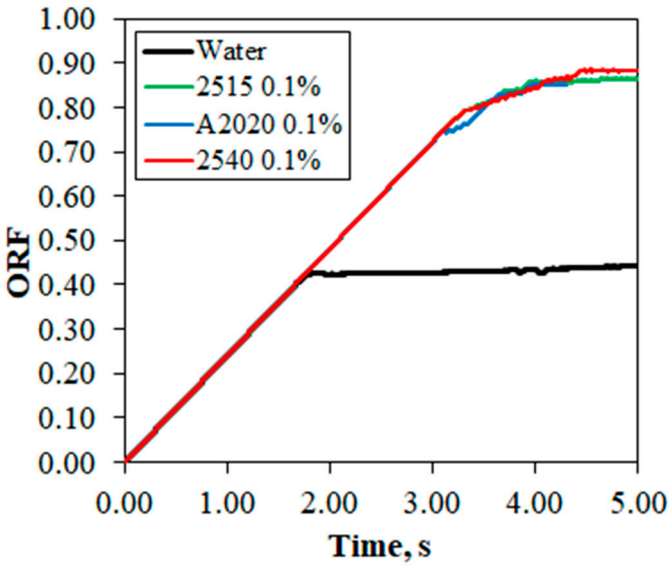

Figure 14. Oil-recovery factor vs. time for polymer solutions with different molecular weights.

In this case, the polymers used are very effective. As you can see, the oil recovery factor for them is close to 90%. A further increase in the displacement ratio is very problematic. And small changes in oil-recovery factors require very large changes in properties. Therefore, the differences between them are not so visible.

3.3. Investigation Influence of the Oil Viscosity

The effect of oil viscosity on the oil-recovery factor (ORF) and pressure drop has been studied when using various displacing agents. Calculations were carried out for water and a polyacrylamide polymer solution with a molecular weight of ~9 mln c.u. at a weight concentration of 0.1%. Rheological parameters, wetting angle, and surface-tension coefficient for this polymer solution were determined experimentally. Calculations were performed for the capillary number of 4×10^{-5}. In the calculations, the oil density was equal to 900 kg/m^3 and the oil-viscosity values were equal to 0.0157 and 0.1 Pa×s, which, respectively, corresponded to high-viscosity oil and extra viscous oil.

A comparison of oil-displacement patterns using water and 0.1% polyacrylamide solution from the fractured medium model is shown in Figure 15. Blue color shows the pore space filled with oil, red is the displacing agent, and white color corresponds to solid rock. It can be seen that, for both considered oil viscosities, in contrast to displacement by water, the displacement using a polymer solution occurs through a wide displacement front covering the entire computational domain, whereas, after displacement by water, especially for high-viscosity oil, many existing zones of pore space filled with oil are not involved in the displacement process.

Quantitative estimation of the calculation results can be done by graphs representing the ORF depending on the weight concentration of the polymer for two values of oil viscosity (see Figure 16a). As can be seen from the graph shown in Figure 16a, the largest increment of the oil-recovery factor, when using a polymer solution, is observed for oil with a higher viscosity (0.1 Pa×s), compared to that for using water. The recovery factor of high-viscosity oil by water was 0.468 while using a polymer solution allowed obtaining ORF equal to 0.88. For oil with a lower viscosity (0.0157 Pa×s), the increment of the ORF when using polyacrylamide solution is less significant compared to that for using water; the oil-recovery factor is 0.784. Using a polymer solution for oil displacement allows obtaining an ORF equal to 0.98. The difference in the increment of the ORF is due to the fact that high-viscosity oil is well-enough displaced by water.

In the course of calculations, the dependences on the pressure drop during oil displacement with water and polymer solutions having different viscosities were obtained (Figure 16b). The pressure drop was determined at a steady section of the displacement process providing a constant value of the ORF. During oil displacement, the pressure drop increases due to both an increase in oil viscosity and the high viscosity of the polymer solution. When displaced by water, an increase in the oil viscosity leads to an increase in the pressure drop by 2.13 times. For an oil viscosity equal to 0.0157 Pa×s, when displaced by a polymer solution, the pressure drop is 17.7 times higher than that for water. With an increase in the oil viscosity, the difference in the pressure drop between the polymer solution and water decreases. Thus, at an oil viscosity of 0.1 Pa×s, the pressure drop for a polymer solution is 11 times higher than that for water.

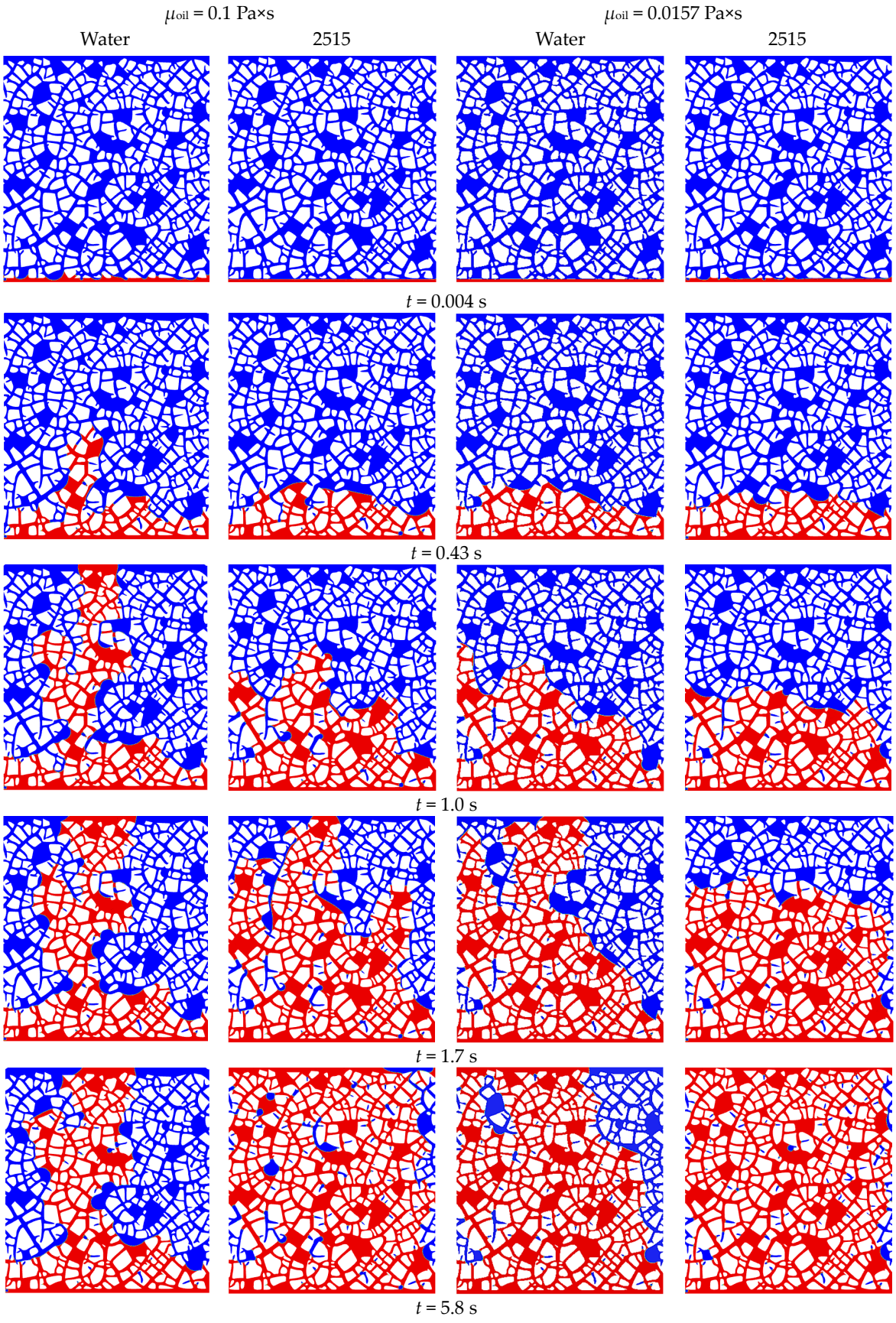

Figure 15. Phase distribution of the displacing agent and oil in a fractured medium during the displacement process. Effect of viscosity oil.

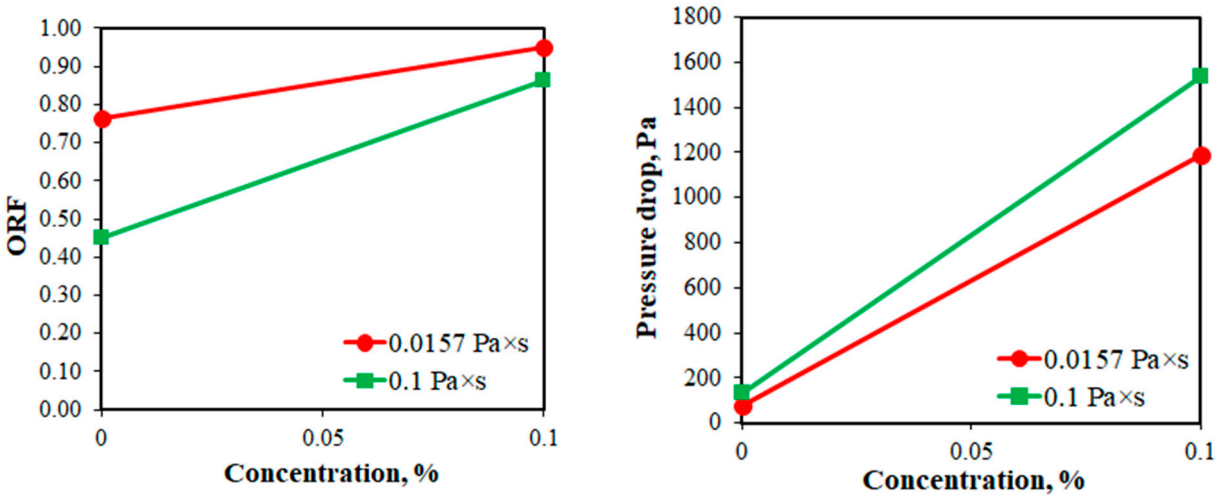

(**a**) (**b**)

Figure 16. The oil recovery (**a**) and the pressure drop (**b**) vs. weight concentration of polyacrylamide for different oil viscosities.

4. Conclusions

Polymer flooding with aqueous solutions of polyacrylamides is today one of the most effective and cheapest polymers used for reservoir flooding. In addition to its availability, other important advantages of polyacrylamides are their good solubility in water, due to which the viscosity of solutions quickly changes, the ability to easily filter in rock, and, also, environmental safety. Despite the fact that polymer flooding has been successfully used in field development for quite a long time, tasks related to optimizing the composition, increasing stability, reducing costs, and reducing the risks of the field-development process are still relevant.

1. A computational study of oil displacement from a fractured medium model obtained by digitizing the image of a fractured surface was carried out. To prepare a naturally cracked structure, an original approach was used, based on the evaporation of a suspension of nanodiamonds on a glass substrate. This made it possible to obtain a topology of the pore space close to the topology of real fractured cavernous rocks. Calculations were performed for solutions of polyacrylamide polymer with different molecular weights. Experimentally determined properties of polymer solutions (viscosity, contact angle at the polymer–oil–rock, and interfacial tension) were used in the model. The computational study was employed to refine the technology for developing fractured structure models. The developed mathematical model was used to obtain new information about the flow of polymer solutions in a fractured medium;
2. The effect of polyacrylamide with a molecular weight of 20 million c.u. at 0.05 and 0.1% for oil displacement during polymer flooding of a fractured medium model. It is shown that using polymer solutions enhances the oil-recovery factor from the fractured medium from 0.45 (when displaced by water) to 0.74 when displaced by a polymer solution with a weight concentration of 0.05%. A further increase in the concentration to 0.1% leads to an enhancement of the oil-recovery factor to 0.85. Such a significant enhancement of the oil-recovery factor is due to the fact that the viscosity of polymer solutions increases significantly compared to that of water, as well as the fact that these solutions are non-Newtonian fluids (whose viscosity coefficient depends on the shear rate);
3. Investigation of the oil displacement from a fractured medium has been conducted for polymers with different molecular weights. Three polyacrylamide polymer solutions with a weight concentration of 0.1% were considered. Grades 2515, 2540, and 2020 polymer solutions with relative molecular weights of 10, 14, and 20 mln c.u. were

considered in the computational study. For the considered 2515, 2020, and 2540 polymer solutions, the oil-recovery factors obtained during calculations were quite similar. The maximum magnitude of the oil-recovery factor for grade 2540 polymer was 0.88, which corresponded to the maximum values of the effective viscosity among the polymer solutions considered. The dependences of the pressure drop for polymers of different molecular weights were obtained. It was revealed that using polymer solutions leads to an increase in the pressure drop by 10 or more times. Thus, the greatest increase in the pressure drop was noted for the grade 2540 polymer solution, which exceeded that for water by 14 times. For grades 2515 and 2020 polymer solutions, the pressure drop was, respectively, 11.4 and 10.8 times greater than that for water;

4. The influence of oil viscosity on the oil-recovery factor and pressure drop during oil displacement using a polymer solution has been studied. Calculations were conducted for a polyacrylamide polymer solution with a molecular weight of 10 mln c.u. at a weight concentration of 0.1%. The largest increment of the oil-recovery factor, when using a polymer solution was observed for high-viscosity oil. During the calculations, the dependences of the pressure drop during the displacement of oil having different viscosities with water and polymer solution were obtained. When using a polymer solution, the pressure drop increased for all the considered oil viscosity coefficients.

The approach used in this work for creating naturally fractured structures seems to us very promising, since it can be a good approximation to the structure of the pore space of real rocks. In the future, it is planned to expand it to the technology of manufacturing microfluidic chips for studying oil recovery.

Author Contributions: D.G.: Conceptualization, Investigation, Writing—original draft. A.S.: Writing—original draft, experimental measure. S.I.: Investigation, Writing—original draft. A.M.: Conceptualization, Writing—original draft, Project administration, Funding acquisition. All authors have read and agreed to the published version of the manuscript.

Funding: This work was supported by the Ministry of Science and Higher Education of the Russian Federation (SFU, No. FSRZ-2020-0012).

Institutional Review Board Statement: Not applicable.

Informed Consent Statement: Not applicable.

Data Availability Statement: Data is contained within the article.

Conflicts of Interest: The authors declare no conflict of interest. The funders had no role in the design of the study; in the collection, analyses, or interpretation of data; in the writing of the manuscript; or in the decision to publish the results.

Nomenclature

μ	Viscosity [Pa·s]	n	Flow-behavior index
ρ	Density [kg/m^3]	K	consistency index [mPa×s]
Ca	Capillary number	$\vec{V}$	Velocity vector
α	Volume fraction	σ	Interfacial tension coefficient [N/m]
θ	Wettability angle at the wall [deg]	φ	Mass concentration of polymer
p	Pressure [Pa]	$\dot{\gamma}$	Shear rate [1/s]
ORF	Oil-recovery factor	p, o	Index polymer and oil

References

1. Firozjaii, A.M.; Saghafi, H.R. Review on chemical enhanced oil recovery using polymer flooding: Fundamentals, experimental and numerical simulation. *Petroleum* **2020**, *6*, 115–122. [CrossRef]
2. Scott, A.J.; Romero-Zerón, L.; Penlidis, A. Evaluation of Polymeric Materials for Chemical Enhanced Oil Recovery. *Processes* **2020**, *8*, 361. [CrossRef]

3. Ibatullin, R.; Gaffarov, S.; Khisametdinov, M.; Minikhairov, L. Review of world polymer flooding EOR projects. *Oil Ind. J.* **2022**, *7*, 32–37. [CrossRef]
4. Moradi-Araghi, A.; Doe, P.H. Hydrolysis and Precipitation of Polyacrylamides in Hard Brines at Elevated Temperatures. *SPE Reserv. Eng.* **1987**, *2*, 189–198. [CrossRef]
5. Levitt, D.B.; Pope, G.A.; Jouenne, S. Chemical Degradation of Polyacrylamide Polymers under Alkaline Conditions. In Proceedings of the 2010 SPE Improved Oil Recovery Symposium, Tulsa, OK, USA, 24–28 April 2010; pp. 970–978.
6. El-Hoshoudy, A.; Desouky, S.; Al-Sabagh, A.; Betiha, M.; El-Kady, M.Y.; Mahmoud, S. Evaluation of solution and rheological properties for hydrophobically associated polyacrylamide copolymer as a promised enhanced oil recovery candidate. *Egypt. J. Pet.* **2017**, *26*, 779–785. [CrossRef]
7. Mishra, S.; Bera, A.; Mandal, A. Effect of Polymer Adsorption on Permeability Reduction in Enhanced Oil Recovery. *J. Pet. Eng.* **2014**, *2014*, 395857. [CrossRef]
8. Li, F.; Zhu, W.-X.; Yu, D.-Z.; Song, H.; Wang, K.-L. Rheological properties and enhanced oil recovery performance of a novel sulfonate polyacrylamide. *J. Macromol. Sci. Part A Pure Appl. Chem.* **2018**, *55*, 449–454. [CrossRef]
9. Abidin, A.; Puspasari, T.; Nugroho, W. Polymers for Enhanced Oil Recovery Technology. *Procedia Chem.* **2012**, *4*, 11–16. [CrossRef]
10. Ghoumrassi-Barr, S.; Aliouche, D. A Rheological Study of Xanthan Polymer for Enhanced Oil Recovery. *J. Macromol. Sci. Part B* **2016**, *55*, 793–809. [CrossRef]
11. Torsæter, O. Application of Nanoparticles for Oil Recovery. *Nanomaterials* **2021**, *11*, 1063. [CrossRef]
12. Hu, Y.; Zhao, Z.; Dong, H.; Mikhailova, M.V.; Davarpanah, A. Hybrid Application of Nanoparticles and Polymer in Enhanced Oil Recovery Processes. *Polymers* **2021**, *13*, 1414. [CrossRef]
13. Davarpanah, A. Parametric Study of Polymer-Nanoparticles-Assisted Injectivity Performance for Axisymmetric Two-Phase Flow in EOR Processes. *Nanomaterials* **2020**, *10*, 1818. [CrossRef]
14. Haruna, M.A.; Gardy, J.; Yao, G.; Hu, Z.; Hondow, N.; Wen, D. Nanoparticle modified polyacrylamide for enhanced oil recovery at harsh conditions. *Fuel* **2020**, *268*, 117186. [CrossRef]
15. Hu, Z.; Haruna, M.; Gao, H.; Nourafkan, E.; Wen, D. Rheological Properties of Partially Hydrolyzed Polyacrylamide Seeded by Nanoparticles. *Ind. Eng. Chem. Res.* **2017**, *56*, 3456–3463. [CrossRef]
16. Loaiza, C.S.; Patiño, J.F.; Mejía, J.M. Numerical evaluation of a combined chemical enhanced oil recovery process with polymer and nanoparticles based on experimental observations. *J. Pet. Sci. Eng.* **2020**, *191*, 107166. [CrossRef]
17. Zhao, W.; Cui, H.; Wang, K. Numerical Calculation of Transient Flow of Polymer Foam in Porous Media. *Open J. Fluid Dyn.* **2015**, *5*, 215–223. [CrossRef]
18. Druetta, P.; Tesi, P.; De Persis, C.; Picchioni, F. Methods in Oil Recovery Processes and Reservoir Simulation. *Adv. Chem. Eng. Sci.* **2016**, *6*, 399–435. [CrossRef]
19. Ambekar, A.S.; Mattey, P.; Buwa, V.V. Pore-resolved two-phase flow in a pseudo-3D porous medium: Measurements and volume-of-fluid simulations. *Chem. Eng. Sci.* **2021**, *230*, 116128. [CrossRef]
20. Patel, H.; Das, S.; Kuipers, J.; Padding, J.; Peters, E. A coupled Volume of Fluid and Immersed Boundary Method for simulating 3D multiphase flows with contact line dynamics in complex geometries. *Chem. Eng. Sci.* **2017**, *166*, 28–41. [CrossRef]
21. Minakov, A.V.; Rudyak, V.Y.; Pryazhnikov, M.I. Systematic Experimental Study of the Viscosity of Nanofluids. *Heat Transf. Eng.* **2020**, *42*, 1024–1040. [CrossRef]
22. Minakov, A.V.; Pryazhnikov, M.I.; Suleymana, Y.N.; Meshkova, V.D. An Experimental Study of the Effect of the Addition of Silicon Oxide Nanoparticles on the Wettability Characteristics of Rocks with Respect to Oil. *Tech. Phys. Lett.* **2020**, *46*, 1238–1240. [CrossRef]
23. Hirt, C.W.; Nichols, B.D. Volume of fluid (VOF) method for the dynamics of free boundaries. *J. Comput. Phys.* **1981**, *39*, 201–225. [CrossRef]
24. Osher, S.; Sethian, J.A. Fronts propagating with curvature-dependent speed: Algorithms based on Hamilton-Jacobi formulations. *J. Comput. Phys.* **1988**, *79*, 12–49. [CrossRef]
25. Gavrilov, A.A.; Minakov, A.V.; Dekterev, A.A.; Rudyak, V.Y. Numerical algorithm for fully developed laminar flow of a non-Newtonian fluid through an eccentric annulus. *J. Comput. Technol.* **2012**, *17*, 44–56.
26. Brackbill, J.; Kothe, D.; Zemach, C. A continuum method for modeling surface tension. *J. Comput. Phys.* **1992**, *100*, 335–354. [CrossRef]
27. Guzei, D.; Zhigarev, V.; Rudyak, V.; Ivanova, S.; Minakov, A. Effect of Initial Water Saturation on Oil Displacement Efficiency by Nanosuspensions. *Fluids* **2022**, *7*, 59. [CrossRef]

Disclaimer/Publisher's Note: The statements, opinions and data contained in all publications are solely those of the individual author(s) and contributor(s) and not of MDPI and/or the editor(s). MDPI and/or the editor(s) disclaim responsibility for any injury to people or property resulting from any ideas, methods, instructions or products referred to in the content.